Lightning Performance of Transmission Lines

Elisa Simões Dias Almeida Abrantes, 72743

Instituto Superior Técnico

***Abstract*—One of the main causes of interruption of electrical power supply is the incidence of lightning in overhead power transmission lines. It is possible to determine the line performance through the calculation of two rates: the shielding failure flashover rate (SFFOR) and the backflashover rate (BFR). This dissertation has the objective of creating a computer program that will take into account all existing methods for calculating the two aforementioned rates, in order to understand the influence of the methods in the results and allow the user to choose which method he believes to be more appropriate. The program was initially based on the methods proposed by IEEE and used on its FLASH program, and was later expanded to include methods from CIGRÉ, and other authors and researchers. All the criteria, models and methods of calculation in which the computer program is based on are described in this work, and various tests of every model and tower type are done. By analyzing the results obtained through various tests it is possible to understand that there are several factors not considered in FLASH that affect the results of SFFOR and BFR, especially for high values of footing resistance. Nonetheless, the results obtained using the FLASH methodology are still considered to be acceptable for most situations.**

***Index Terms*—BFR, FLASH, flashover, lightning, SFFOR**

I. Introduction

In high voltage, energy transmission is done in overhead lines that are exposed to various factors that may lead to the occurrence of defects which can cause an interruption in the electricity supply.

Of the factors that may cause defects, the largest contributor is the lightning stroke. Being a natural phenomenon, it is impossible to prevent its occurrence, but it is possible to estimate the performance of transmission lines to lightning, and plan its construction in order to minimize the effects of the lightning discharge.

The performance of overhead transmission lines is measured by the number of lightning that reach a line component and cause a flashover. According to [5], if the lightning hits a phase conductor and causes flashover on the insulators, then there was a shielding failure, and it is necessary to calculate the SFFOR, that indicates the number of lightning that hit the line, in 100 km of line, in a year, that lead to a flashover. If the lightning hits the shield wires or the tower, then there is an overvoltage that may be high enough to cause the backflashover of the isolators. In this case it is necessary to find the BFR, that shows the number of lightning, in 100 km of line, in a year, that cause backflashover.

The objective of this work is to create a computer program that considers all the possible methods of calculating the rates mentioned before, in order to verify if the currently used methods are the most beneficial to use and if not, what would be the preferred alternatives.

To start this process, the IEEE program, FLASH, is analyzed, and a base program is created. Afterwards, the alternative methodologies for the calculation of the rates, proposed by CIGRÉ and other authors, are considered. Finally, a study of different methods for intermediate calculations and different parameters is made. The program created is presented and in the last chapter of this work the tests made and results obtained are discussed.

II. Base Methodology

The base program considers all models and parameters used in FLASH, and aims to recreate it. This program indicates the values of SFFOR and BFR, thereby allowing us to analyze the lightning performance of the line.

A. The Lightning Stroke

Lightning is a disruption of the air that occurs when a *cumulo nimbus* cloud is electrified. The *cumulo nimbus* is a cloud with considerable height, situated from 2 km above the ground and stretching up to 20 km above the ground. The disruption can occur between differently charged regions of the cloud (intra-cloud lightning), between two clouds (inter-cloud lightning), or between the cloud and the ground. Lightning is further classified by its polarity (negative or positive), and by its direction (upwards or downwards).

The discharge is created in three steps. Considering a downward stroke, firstly a downward leader leaves the cloud with a certain charge. With its approach to ground, the electric field in the ground grows, until it becomes high enough for an upward leader to move up in the direction of the downward leader. When the two leaders meet, a conducting path is created, leading to an electrical discharge called “return stroke” that can be seen as a bright flash of light.

B. Keraunic Activity

To be able to evaluate the lightning performance of a line, it is necessary to know the keraunic activity of the region. The keraunic activity relates to how many lightning strikes hit a certain region, and can be measured by two indexes: the

This work was submitted on October of 2016 and was supervised by Professor Maria Teresa Nunes Padilha de Castro Correia de Barros.

Elisa Abrantes is a Master student at Instituto Superior Técnico of the Universidade de Lisboa, in Lisbon Portugal.

keraunic level, T_d, which indicates the number of thunderstorms days per year, and the hourly keraunic level, T_h, that indicates the number of thunderstorm hours per year.

In a practical use, and especially considering the approach followed by FLASH, the most important quantity is the ground flash density (GFD) N_g, that indicates the number of lightning strikes to ground in a year, per 100 km^2. If the GFD is not an available data for the region, it may be calculated by (1) or (2).

$$N_g = 0.04{T_d}^{1.25} \tag{1}$$

$$N_g = 0.054{T_h}^{1.1} \tag{2}$$

Knowing the GFD allows us to find the flash collection rate N_L, the number of flashes to the line, per 100 km of line, per year.

$$N_L = \frac{N_g}{10}\left(28{h_t}^{0.6} + b\right) \tag{3}$$

Where h_t is the tower height and b is the distance between shield wires.

C. *Modeling Components*

Let us now consider all the components necessary to calculate the SFFOR and BFR.

1) *Stroke Current*

Seeing as the lightning stroke is a purely natural and random phenomenon, it is only possible to describe it with probabilistic distributions obtained through experimental studies. According to [1], the probability density, $f_1(I)$,of the stroke current, I_f, is given by a log normal distribution.

$$f(I) = \frac{1}{\sqrt{2\pi}\sigma_{log}I} e^{-\frac{\ln\left(\frac{I}{M}\right)^2}{2{\sigma_{log}}^2}} \tag{4}$$

Where σ_{log} is the standard deviation and M is the mean.

However, the IEEE in FLASH uses another curve, obtained through experimental results. The cumulative probability of I_f exceeding I for this curve is approximated by (5) for currents between 5 kA and 200 kA.

$$P(I > I_f) = \frac{1}{1+\left(\frac{I_f}{I_{first}}\right)^{2.6}} \tag{5}$$

Where I is in kA and $\bar{I}_{first}$ is 31 kA.

2) *Phase conductors*

The flash program takes into account the corona effect in the conductor or shield wire radius. The radius of the corona envelope may be calculated by an iterative process.

$$R_{cor}^{n+1} = \frac{U_{crit}}{E_0 \ln\left(\frac{2h_{av}}{R^n}\right)} \tag{6}$$

Where $R_{cor}$is the radius of the corona envelope in (m), h_{av} is the average height of the phase conductor or shield wire (m), U_{crit} is the flashover voltage in the insulator (kV), and $E_0$is the limiting corona gradient below which the envelope can no longer grow (1500 kV/m) [3].

The average height of a phase conductor or shield wire is given by (7), where h is the conductor or shield wire height (m) and S_f is the sag (m).

$$h_{av} = h - \tfrac{2}{3}S_f \tag{7}$$

In the case of bundle conductors, it is necessary to reduce them to an equivalent single conductor, using (8). According to [3] this is done assuming that the equivalent conductor will carry the same charge and voltage to ground as the bundle and will be located where the center of the bundle was located.

$$R_{eq\_bundle} = \sqrt[N]{r_{11}r_{12}r_{13} \dots r_{1N}} \tag{8}$$

Where R_{eq_bundle} is the radius of the equivalent conductor (m), r_{11} is the radius of subconductor 1, r_{12} is the distance from conductor 1 to conductor 2, and N is the number of subconductors.

The final radius, R_{eq_Total}, of the conductor, needed to calculate its impedance, is given either by (10), in case of bundle conductors, or (11) in case of a single conductor.

$$R_{eq\_Total} = R_{cor} + R_{eq\_bundle} \tag{9}$$

$$R_{eq\_Total} = R_{cor} \tag{10}$$

The self-surge impedance of a single conductor in heavy corona is given by

$$Z_{c\_nn} = 60\sqrt{\ln\left(\frac{2h_{cav\_n}}{r_n}\right)\ln\left(\frac{2h_{cav\_n}}{R_{eq\_Total\_n}}\right)} \tag{11}$$

where Z_{c_nn} is the self-surge impedance of conductor n (Ω), h_{cav_n} is the average height of conductor n (m), r_n is the radius of the conductor n without corona effect (m), and $R_{eq\_Total\_n}$ is the radius of the conductor n with corona effect (m).

3) *Shield Wires*

The self-surge impedance of a shield wire can be given by (12), which is simply the shield wire version of (11), where Z_{g_nn} is the self-surge impedance of shield wire n (Ω), h_{gav_n} is the average height of shield wire n (m), r_{g_n} is the radius of the shield wire n without corona effect (m), and $R_{eq\_gTotal\_n}$ is the radius with corona effect (m).

$$Z_{g\_nn} = 60\sqrt{\ln\left(\frac{2h_{gav\_n}}{r_{g\_n}}\right)\ln\left(\frac{2h_{gav\_n}}{R_{eq\_gTotal\_n}}\right)} \tag{12}$$

In case of the existence of two shield wires, it is proposed by [3] that the two shield wires impedances should be reduced to an equivalent single-wire impedance.

$$Z_g = \frac{Z_{11}+Z_{12}}{2} \tag{13}$$

Where Z_{11} is the self-surge impedance and Z_{12} is the mutual impedance between two shield wires. The mutual impedance can be found by:

$$Z_{g\_mn} = 60\ln\left(\frac{a_{mn}}{b_{mn}}\right) \tag{14}$$

where a_{mn} is the distance from shield wire m to the image of n in the earth, and b_{mn} is the direct distance between m and n.

According to [3], the portion of stroke current that flows through the shield wires induces a voltage in each phase conductor. The ratio between the induced voltage in the conductor and the tower top voltage is the coupling factor. This factor can be calculated by (15), if there are two shield wires, or (16), if there is only one shield wire.

$$K_n = \frac{Z_{n1}+Z_{n2}}{Z_{11}+Z_{12}} \quad (15)$$

$$K_n = \frac{Z_{n1}}{Z_{11}} \quad (16)$$

4) Tower

According to [1] the FLASH program allows the user to choose between four different towers shapes: 1-Conical; 2-H-Frame; 3-Cylindrical; 4-Waist. In [8] these same towers are given the following names: 1-Sargent's Cone; 2-H shape; 3-Hileman's cylinder; 4-Chisholm's belt. The shapes and impedance formulas of this towers are shown in the following figures.

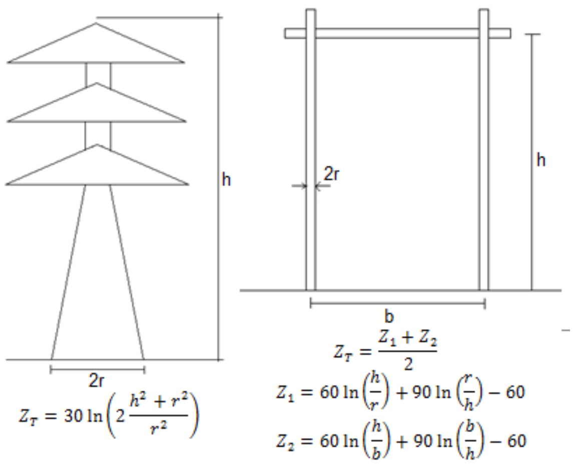

Fig. 1. Tower shapes and impedance equations for Sargent's cone (left) and H shape (right).

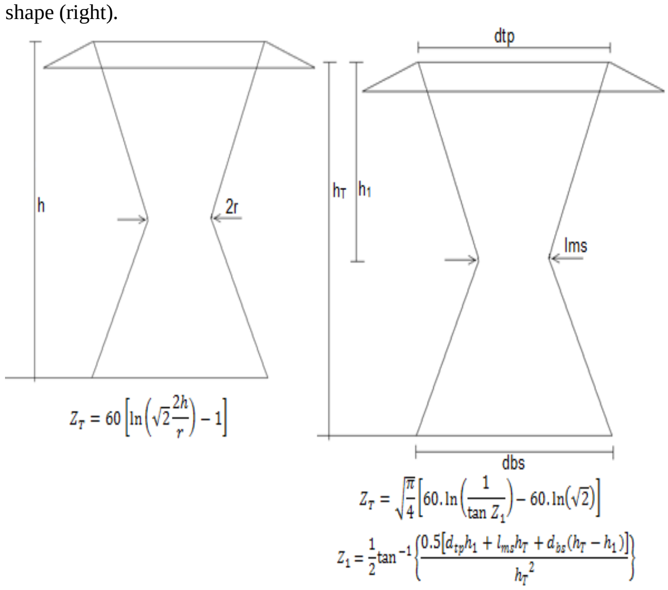

Fig. 2. Tower shapes and impedance equations for Hileman's cylinder (left) and Chisholm's belt (right).

5) Tower to ground connection

The tower to ground connection is made by electrodes, that allow the discharge currents to flow from the tower to the ground, avoiding damage to equipment and assuring the safety of people and animals [5]. The simplest way of representing the electrode is by the footing resistance, R_T, which is a parameter that can be influenced by various factors, such as stroke current, soil humidity, type of soil and soil ionization. The FLASH program does not consider the effect of soil ionization, but this factor will be taken into account later in this work.

6) Isolators

According to [1], the critical voltage for the disruption of the isolators is calculated in kV by

$$U_{crit}(t) = \left(400 + \frac{710}{t^{0.75}}\right) l_d \quad (17)$$

where t is the time in microseconds and l_d is the size of the isolator chain (m) or of the air interval, whichever is smaller.

In the calculation of the SFFOR, it is considered by [3] that the time until flashover is 6 μs, and therefore (17) may be simplified to (18), to be used both for the calculation of the corona envelope and the critical current. For the BFR, the calculation of the corona envelope should take into account 2 μs, resulting in (19), whereas for the calculation of the critical current we must take into account the smallest value of the critical voltage, between 2 μs and 6 μs.

$$U_{crit}(6\mu s) = 585 l_d \quad (18)$$

$$U_{crit}(2\mu s) = \begin{cases} 820 l_d, \ \tau_s < 1\mu s \\ \left(400 + \frac{710}{(2\tau_s)^{0.75}}\right) l_d, \ \tau_s \geq 1\mu s \end{cases} \quad (19)$$

Where τ_s is travel time in the span, that depends on the length of the span, l_v, and c is the speed of light.

$$\tau_s = \frac{l_v}{c \times 0.9} \ [\mu s] \quad (20)$$

D. The SFFOR

The calculation of the SFFOR requires several steps, here explained.

1) Critical current

The flashover of the isolators can only occur if the discharge current is high enough. The minimum current that can lead to flashover is given by

$$I_c = 2\frac{U_{crit}(6\mu s)}{Z_c} \quad (21)$$

Where U_{crit} is the critical voltage and Z_c is the conductor impedance.

2) Phase Conductor Exposure

When lightning approaches the line, the phase conductor is not exposed in its entirety. The length of conductor exposed varies with the height of the conductors and shield wires, and with the stroke current. To find the exposure, D_c, the IEEE uses the electro-geometric model (EGM), exemplified in Fig. 3, to calculate the striking distance to the conductor r_c, and the striking distance to ground, r_g.

$$r_c = AI^B \quad (22)$$

$$r_g = \beta r_c \quad (23)$$

$$\beta = \frac{22}{h_{cav}} \quad (24)$$

Where IEEE proposes, in [9], A=8 and B=0.65.

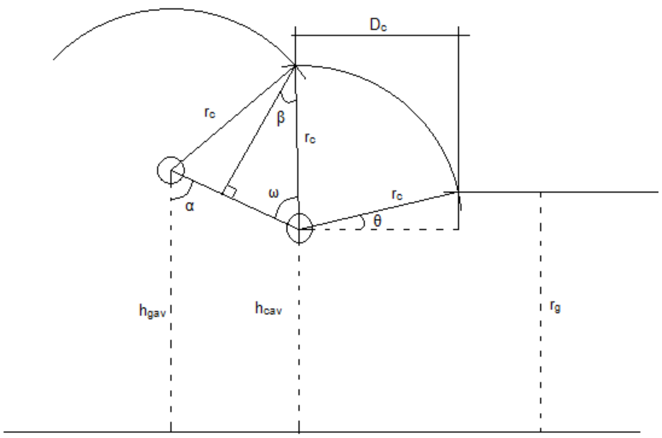

Fig. 3. EGM to determine the exposure of the phase conductors to lightning.

With this values it is possible to find the exposure, through the following steps, as shown in [3].

$$\theta = \sin^{-1}\left(\frac{r_g - h_{cav}}{r_c}\right) \tag{25}$$

$$\alpha = \tan^{-1}\left(\frac{x_c - x_g}{h_{gav} - h_{cav}}\right) \tag{26}$$

$$\omega = \cos^{-1}\left(\frac{\sqrt{(x_c - x_g)^2 + (h_{gav} - h_{cav})^2}}{2r_c}\right) \tag{27}$$

$$D_c = \begin{cases} r_c[1 + \sin(\alpha - \omega)],\ r_g < h_{cav} \\ r_c[\cos(\theta) + \sin(\alpha - \omega)],\ r_g \geq h_{cav} \end{cases} \tag{28}$$

3) *Maximum current*

With the raise of the stroke current, the exposure diminishes. The maximum current, I_{max}, is the one that leads to no exposure, and maximum striking distance. To find I_{max} we must first find its corresponding striking distance, and then use (22) to find the current.

According to [3], the maximum striking distance may be found by geometric analysis of the EGM, following the steps indicated below:

$$r_{c\_max} = -Y_0 \frac{1}{\frac{TM}{\sqrt{1+TM^2}} - \beta} \tag{29}$$

Where TM and Y_0 are given by

$$TM = \frac{|x_c - x_g|}{h_{gav} - h_{cav}} \tag{30}$$

$$Y_0 = \frac{h_{gav} + h_{cav}}{2} \tag{31}$$

Where x_c and x_g are the horizontal coordinates of the phase conductor and the shield wire (m), and h_{cav} and h_{gav} are the average heights of the conductor and shield wire.

4) *Shielding Failure Flashover Rate*

According to [1] and [7], the value of the SFFOR can be found by (32), an equation that uses (4). However, it is possible to simplify this equation by using (5) instead, obtaining (33).

$$SFFOR = 2\frac{N_g}{10}\int_{Ic}^{Imax} D_c(I) f(I) dI \tag{32}$$

$$SFFOR = 2\frac{N_g}{10}\frac{D_c}{2}\left(P_{I_c} - P_{I_{max}}\right) \tag{33}$$

Where P_{I_c} is the probability of the stroke current being higher than the critical current, $P_{I_{max}}$ is the probability of the stroke current being higher than the maximum current, and $D_c/2$ is the average value of the exposure, with D_c calculated for the critical current given by (21).

E. The BFR

For the calculation of the BFR we consider that all the lightning that hit the shield wires hit the tower instead. Due to this, it is necessary to apply a correcting factor that represents the decrease that the strikes suffer, from the middle of the span to the tower. According to [7], this factor must be 0.6.

1) *Tower Voltage*

According to [3] the tower top voltage in kV is given by

$$V_T(t) = Z_I I(t) - Z_w \sum_{n=1}^{N} I(t - 2n\tau_T)\psi^{n-1}. \tag{34}$$

Where Z_I is the intrinsic circuit impedance (Ω):

$$Z_I = \frac{Z_g Z_T}{Z_g + 2Z_T}. \tag{35}$$

Z_w is the constant wave impedance (Ω), given by

$$Z_w = \left[\frac{2{Z_g}^2 Z_T}{(Z_g + 2Z_T)^2}\right]\left[\frac{Z_T - R_T}{Z_T + R_T}\right]. \tag{36}$$

ψ is a damping constant that successively reduces the contribution of reflections, given by

$$\psi = \left(\frac{2Z_T - Z_g}{Z_g + 2Z_T}\right)\left(\frac{Z_T - R_T}{Z_T + R_T}\right). \tag{37}$$

τ_T is the travel time in microseconds from tower top to base.

$$\tau_T = \frac{h_T}{c} \quad [\mu s]. \tag{38}$$

And N is the number of reflected waves, for which the largest value will be the largest whole number that validates $N \leq t/2\tau_T$.

As stated before, the FLASH considers two moments for the occurrence of backflashover: 2 μs and 6 μs. The moment chosen to calculate the BFR will be the one with the lowest critical current. Knowing this, it is necessary to calculate all tower voltages to these two moments.

Considering a stroke current of 1 kA, the tower top voltage is given by

$$V_T(2\mu s) = \left[Z_I - \frac{Z_w}{1-\psi}\left(1 - \frac{\tau_T}{1-\psi}\right)\right].1. \tag{39}$$

$$V_T(6\mu s) = \left[\frac{Z_g R_T}{Z_g + 2R_T}\right].1. \tag{40}$$

It is necessary to take into account the waves reflected in the neighboring towers and that arrive at the hit tower at the moment *t*. This waves introduce the component (41), where $\bar{\beta}_s$ is the reflecting factor in the span. Considering (41) only for the two moments in study we obtain (42) and (43).

$$V'_T(t) = \bar{\beta}_s V_T(1 - 2\tau_S) \tag{41}$$

$$V'_T(2\mu s) = \frac{-4K_S[V_T(2\mu s)]^2}{Z_g}\left[1 - \frac{2V_T(2\mu s)}{Z_g}\right](1 - \tau_S) \tag{42}$$

$$V'_T(6\mu s) = -4K_S Z_g \left[\frac{R_T}{Z_g+2R_T}\right]^2 \left[1 - \frac{2R_T}{Z_g+2R_T}\right]. \quad (43)$$

Where K_S is an attenuating factor for which [3] assumes the value 0.85. The same author also states that if $\tau_S > 1\mu s$ then $V'_T(2\mu s) = 0$.

The final value of the tower top voltage will be

$$\bar{V}_T = V_T + V'_T. \quad (44)$$

The voltage in the footing resistance, simplified to 2 μs and 6 μs is given by

$$V_R(2\mu s) = \frac{\alpha_R Z_I}{1-\psi}\left(1 - \frac{\psi \tau_T}{1-\psi}\right).1 \quad (45)$$

$$V_R(6\mu s) = V_T(6\mu s) \quad (46)$$

Where α_R is

$$\alpha_R = \frac{2R_T}{Z_g+R_T}. \quad (47)$$

The voltage at the crossarm n is given by

$$V_{pn}(2\mu s) = V_R(2\mu s) + \frac{\tau_T - \tau_{pn}}{\tau_T}[V_T(2\mu s) - V_R(2\mu s)] \quad (48)$$

$$V_{pn}(6\mu s) = V_T(6\mu s) \quad (49)$$

Where τ_{pn} is the time from tower top to crossarm, given by (52) where h_T h_{pn} is height of the crossarm.

$$\tau_{pn} = \frac{h_T - h_{pn}}{c} \quad [\mu s] \quad (50)$$

Finally, the voltage at the isolators of phase n is given by

$$V_{sn}(2\mu s) = V_{pn}(2\mu s) - K_n \bar{V}_T(2\mu s) \quad (51)$$

$$V_{sn}(6\mu s) = \bar{V}_T(2\mu s)(1 - K_n) \quad (52)$$

2) Critical Current

The critical current for the phase conductor n is given in [3] by (53).

$$I_{cn}(t) = \frac{U_{crit_n}(t)}{V_{sn}(t)} \quad (53)$$

Equation (53) has to be calculated for both 2 μs and 6 μs, and the lowest value must be chosen.

It is now necessary to note that (53) does not take into account the phase-to-ground voltage. This is extremely important since this voltage is different for each phase, and will have a significant influence in the value of the critical current in the phase conductors. To take this into account [3] proposes a method where the period of time that each phase is dominant (when the phase has the lowest current between all the phases) is defined, allowing to calculate an average critical current (55) for each phase.

To do this, we first find the critical current taking into account the ground-to-phase voltage, (54), and find the periods of dominance by finding the proportion of a period (2π) where each phase is dominant, as shown in Fig. 4. It is then possible to find the average critical current during the dominance period using (55).

$$I'_{cn}(t) = \left[\frac{U_{crit_n}(t) - U_{pf}\sin(\theta_n - \alpha_n)}{U_{crit_n}(t)}\right] I_{cn} \quad (54)$$

Where U_{pf} is the ground-to-phase voltage, α_n is the phase angle of phase n (0º, 120º, or 240º), and θ_n is instantaneous angle of the voltage, that defines the limits of the dominance period.

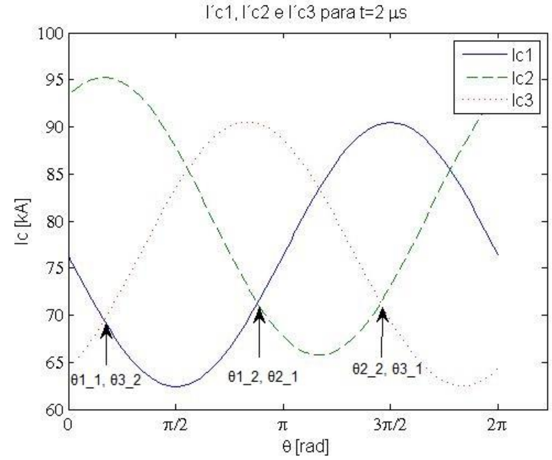

Fig. 4. Critical current and dominant phases

$$I'_{cn_{med}}(t) = \left[1 + \frac{U_{pf}}{U_{crit_n}(t)} \frac{\cos(\theta_2 - \alpha_n) - \cos(\theta_1 - \alpha_n)}{\theta_2 - \theta_1}\right] I_{cn} \quad (55)$$

3) The Backflashover Rate

According to [7], the BFR is given by (56), where I_c is given by (55).

$$BFR = 0.6 N_L \int_{I_c}^{\infty} f(I) dI \quad (56)$$

However, as done in the SFFOR, it is possible to change the stroke current equation from (4) to (5), simplifying (56) into (57), where t_i is the percentage of time each phase is dominant, $P_{I'cn_{med}}$ is the probability of the stroke current being higher than the critical current, and n_c is the number of phases.

$$BFR = 0.6 N_L \sum_{i=1}^{i=n_c} t_i P_{I'cn_{med}} \quad (57)$$

III. Alternative Methodologies

The FLASH program is created by IEEE and therefore utilizes the methodologies proposed and favored by it. This chapter offers a compilation of all the alternative methodologies found by the author. It is divided in two parts: the first refers to calculation methods, the second to different methodologies and models for modeling components.

A. Calculation Methods

In this section we analyze the different methods proposed for the final calculation of the SFFOR and the BFR, as well as the calculation of the critical current of backflashover.

Has shown in previous chapters, there are two methods for calculating both the SFFOR and the BFR. While these methods show many differences, the main difference deals with the stroke current. The IEEE method uses an expression to describe the stroke current that is based on parameters that are different from the ones used on the CIGRE method. This makes it impossible to directly compare the two methodologies. It was therefore necessary in this thesis, to obtain a function related to the one used by IEEE, and implement it in the CIGRE methodology. To do this, we derived (5) and obtained (58). We will now refer to this approach of the CIGRE method using an IEEE stroke current description as the IEEE-D, and to (58) as the IEEE-D curve.

$$f_p(I) = \frac{d}{dI}P(I > I_f) = \frac{D\left(\frac{I}{M}\right)^D}{I\left(1+\left(\frac{I}{M}\right)^D\right)^2} \tag{58}$$

Where $M = 31$ and $D = 2.6$.

1) Methods for Calculating the SFFOR

We have already seen the two equations that we can use to calculate the SFFOR, (32) will use (58) to describe the stroke current and (33) will use (5). The biggest difference between these two methods is the fact that IEEE in (33) considers the average value of the exposure while with IEEE-D in (32) the exposures varies with the stroke current.

2) Methods for Calculating the BFR

Just as in the previous section, the two equations available for the calculation of the BFR have already been shown, they are (56), which uses (58) to describe the stroke current, and (57), which uses (5). In this case, the two methods differ in the fact that the IEEE method, (57), considers the dominant period of each phase, while IEEE-D, (56), considers only the lowest value of the critical current.

It is also possible to consider different methods for calculating the critical current of backflashover.

a) Methods for Calculating the critical current for BFR

The critical current used in the BFR equation comes from the IEEE method shown in the last chapter for the calculation of the critical current. However, CIGRÉ in [7] offers (59) as an alternative

$$I_{cn} = \frac{U_{50ns} - U_{pf}}{R_e(1-K_n)} \tag{59}$$

Where U_{pf} is the ground-to-phase voltage, K_n is the coupling factor, and U_{50ns} and R_e are given by

$$R_e = \frac{Z_g R_i}{Z_g + 2R_i} \tag{60}$$

$$U_{50ns} = \left(0.977 + \frac{2.82}{\tau}\right)U_{50} \tag{61}$$

Where R_i is the footing resistance, Z_g the shield wire impedance, U_{50} the critical voltage in the isolators, and τ is the time constant given by

$$\tau = \frac{Z_g}{R_i}\tau_s \tag{62}$$

It is also possible to consider another, simplified, method. Considering Fig. 5 and the circuit equation (63), [2] declares that if we disregard the propagation time, the voltage drop in the tower, and the reflections of voltage waves in the neighboring towers, it is possible to obtain (64).

TABLE I
PARAMETERS FOR STROKE CURRENT EQUATION (4)

Author	Mean - M	Standard Deviation - σ_{ln}
Berger et al.	31.1	0.484
Anderson-Eriksson	$\begin{cases} 61, & I < 20 \\ 33.3, & I > 20 \end{cases}$	$\begin{cases} 1.33, & I < 20 \\ 0.605, & I > 20 \end{cases}$

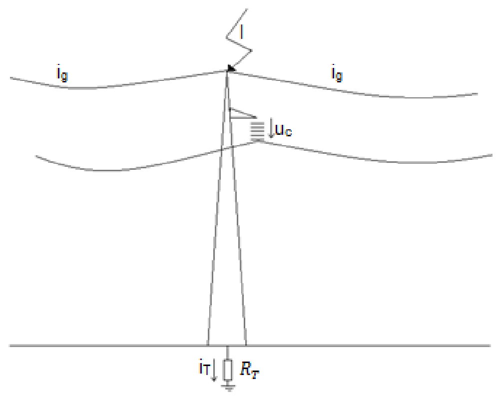

Fig. 5. Division of stroke current.

$$\begin{cases} i = 2i_g + i_t \\ Z_g i_g = R_T i_t \end{cases} \Leftrightarrow \begin{matrix} i_g = \frac{R_T}{Z_g + 2R_T} i \\ i_t = \frac{Z_g}{Z_g + 2R_T} i \end{matrix} \tag{63}$$

$$I_c = \frac{U_{crit} + U_{pf}}{\frac{R_T Z_g}{Z_g + 2R_T}(1-K_n)} \tag{64}$$

B. Modeling Components

This section is dedicated to the different models proposed for various components described in II.B and II.C.

1) Methods for Stroke Current

Considering (4), there are various values for the parameters of this equation. Firstly there is the IEEE-D with (58) as discussed before. Secondly there is the original CIGRÉ method indicated in [7], proposed by Anderson and Eriksson. CIGRÉ also indicates another set of parameters that, according to Nucci [17], were originally proposed by Berger *et al*. The values proposed by these authors can be seen in Table I.

For (5), the parameters indicated in the last chapter are also proposed by Anderson and Eriksson, and the ones used by IEEE. There was another set of values proposed previously by Popolansky, which leads to (65). Both curves were created through the same experimental processes, however, the Popolansky curve was created through a study in which around 50% of the observations were based on chimneys of non-specified height, which lead to unsatisfactory results, and the later study by Anderson and Eriksson that created (5).

$$P(I > I_f) = \frac{1}{1+\left(\frac{I_f}{25}\right)^2} \tag{65}$$

2) Methods for Flash Collection Rate

The equation for the flash collection rate, N_L, given in the last chapter, is the one adopted by IEEE, and was proposed by Eriksson. According to [20], there are two other possible ways of calculating N_L, presented in Table II. One is proposed by

TABLE II
POSSIBLE EQUATIONS FOR THE COLLECTION RATE

Author	N_L [flashes/100 km/year]	
IEEE - Eriksson.	$N_L = \frac{N_g}{10}\left(28{h_t}^{0.6} + b\right)$	
Anderson	$N_L = \frac{N_g}{10}\left(4{h_{cav}}^{1.09} + b\right)$	(66)
Rizk	$N_L = \frac{N_g}{10}\left(38{h_{cav}}^{0.45} + b\right)$	(67)

TABLE III
PARAMETERS TO BE USED FOR STRIKING DISTANCE IN (24) AND (25)

Author	A	B	β
Wagner and Hileman	14.2	0.42	1
Young et al.	*	0.32	**
Armstrong and Whitehead	6.72	0.80	6/6.7
Brown and Whitehead	7.1	0.75	6.4/7.1
Love	10	0.65	1
Whitehead	9.4	0.67	1
Anderson	10	0.65	0.64 – UHV; 0.8 – EHV; 1 – Others
IEEE WG 85	8	0.65	$\frac{22}{h_{cav}}$
IEEE WG 97	*10*	0.65	***

$$*\begin{cases} 27, & h_g < 18m \\ 27\frac{444}{462-h_g}, & h_g > 18m \end{cases} \qquad **\begin{cases} 1, & h_g < 18m \\ \frac{462-h_g}{444}, & h_g > 18m \end{cases}$$

$$***\begin{cases} 3.6 + 1.7\ln(43 - h_c), & h_c < 40m \\ 5.5, & h_c > 40m \end{cases}$$

Anderson, and another is proposed by Rizk.

3) *Methods for Striking Distance*

Considering (22) and (23), there are many possible values for the parameters A, B, and β, as is indicated in [7], [14], and [17]. The most commonly used are the ones proposed by IEEE working groups, IEEE WG 85, used in the base methodology, and IEEE WG 97. All the values proposed by the different authors are presented in Table III.

4) *Consideration of Corona Effect*

As was seen before, the FLASH methodology is one that takes corona effect into account. In order to analyze the difference in results between an approach that considers the corona effect, and one that disregards it, we will now discuss the necessary alterations to the previous equations.

As seen before, the corona effect influences the radius of conductors and shield wires, which will then influence their self-surge impedance. Therefore, we must exchange (11) and (12) with (68) and (69), respectively.

$$Z_{c\_nn} = 60\ln\left(\frac{2h_{cav\_n}}{r_c}\right) \tag{68}$$

$$Z_{g\_nn} = 60\ln\left(\frac{2h_{gav\_n}}{r_g}\right) \tag{69}$$

Where h_{cav_n} and h_{gav_n} are the average heights of the conductor and shield wire of phase n, and r_c and r_g are the radius of the conductor and shield wire, without corona effect.

5) *Methods for Soil Ionization*

While the IEEE does not consider the soil ionization in FLASH, both CIGRÉ [7] and Anderson [3] take it into account. It is therefore important to analyze the two situations.

Soil ionization affects the footing resistance. Both authors propose the same method for calculating the footing resistance when the soil ionization is considered.

$$R_i = \frac{R_T}{\sqrt{1+\frac{I}{I_g}}} \tag{70}$$

$$I_g = \frac{E_g\rho}{2\pi {R_T}^2} \tag{71}$$

Where E_g is the electric field, considered to be 400 kV/m [7], ρ is the soil resistivity (Ω.m), and R_T is the footing resistance without soil ionization (Ω).

6) *Methods for Tower Impedance*

Observing the tower impedances given in Fig. 1 and Fig. 2, it is possible to see that these impedances are all purely resistive. Here we propose to analyze the effect of a purely inductive tower impedance in the results of the BFR.

IV. THE PROGRAM

In order to analyze all the scenarios discussed in previous chapters, a computational program was created, and given the name “LIPE”. It is possible to see in Fig. 6 the interactive window of this program. The user must give all the necessary data as input, choosing the method for calculating N_L (N_g, T_d, or T_h) and the tower shape (type 1 to 4).

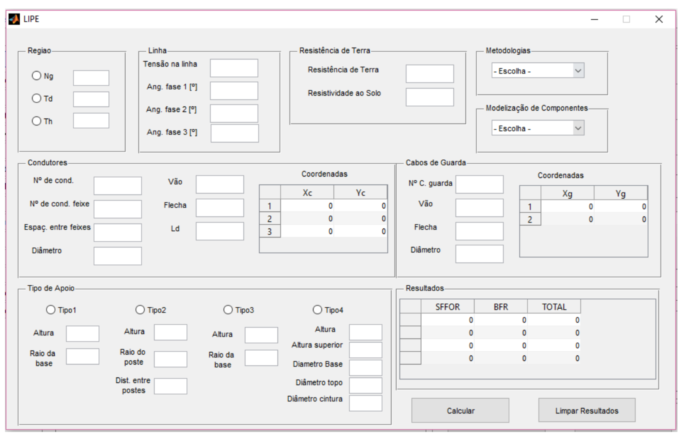

Fig. 6. LIPE user interactive window.

It is also necessary to choose an input from each of the two list menus available. One of the lists is labeled “Metodologias” and has 7 options for methodologies (Base method, Base method with integral, Popolansky method, CIGRÉ method, Berger method, Ic BFR-CIGRÉ, and Ic BFR-simplified). The other list is called “Modelização de componentes” and has 15

TABLE IV
GENERAL DATA

Footing Resistance (Ω)	Rt	25
Ground flash density (disch/km^2/yr.)	Ng	2.2
(Ωm)	ρ	150
Conductor Sag (m)	fc	11.3
Shield wire sag (m)	fg	8.7
Conductor diameter (mm)	dc	31.8
Shield wire diameter (mm)	dg	16
Span (m)	dv	300
Isolator chain width (m)	ld	1.9
220 kV Line with phases:		
Angle Phase1 (º)	alfa1	0
Angle Phase 2 (º)	alfa2	120
Angle Phase 3 (º)	alfa3	240

options for component models (1 for the Base method, 2 for N_L calculation models, 9 for striking distance models, 1 for no corona effect, 1 for soil ionization, and 1 for Tower inductive impedance).

After inserting all the necessary data, it is only necessary to press “Calcular” and the results will appear in the “Resultados” panel, along with the name of the methodology and component models chosen. The first line of the results table will refer to the most recent test, and the following lines will refer to previous tests, form the most recent to the oldest. To clean the results table press “Limpar”.

V. TESTS AND RESULTS

While LIPE allows for a multitude of combinations between the two list menu options, the objective of this work was to compare the FLASH with all other possible methods. Therefore, three types of tests were done. Firstly, LIPE was tested directly in comparison to FLASH, in order to verify that the methodology used was correct. Secondly, to test the calculation methods the option chosen in the first list referring to methodologies was altered in sequence for each test, while the second list referring to component models was kept in the base method. Finally, the inverse process was done to test the component models: the list referring to methodologies was kept in the base method while the option chosen in the list referring to component models was changed in every test.

The general data used for the lines is given in table IV, the data for each type of tower is shown in Table V and the tests done are described in Table VI. Each set of tests was repeated for each of the tower types (except for test 5 which does not apply to tower type 1), before changing the list menu options for the following set. The results can be seen in the Appendix.

It is important to note that while FLASH shows results to the second decimal, LIPE shows to the fourth decimal.

1) *FLASH vs. LIPE*

The results obtained, for the different tower types (Appendix Table A), showed that LIPE allows for a very good approximation to FLASH, when using the base methodology.

TABLE V
DATA FOR TOWER TYPES

Tower type 1		Tower type 2		Tower type 3		Tower type 4	
ht	30	ht	30	ht	30	ht	30
2r	5.2	2r	2	2r	3.8	dbc	2.8
X1	-7	b	12.6	Xc	8	lms	1.9
X2	-6.5	Xc	8	Xg	6.3	dtp	6.3
X3	6.5	Xg	6.3	Yc	23.8	h1	15.6
Y1	13.3	Yc	23.8	Yg	30	Xc	8
Y2	21.3	Yg	30			Xg	6.3
Y3	17.3					Yc	23.8
Yg	30					Yg	30

TABLE VI
TESTS MADE WITH LIPE

Test	
1	Base Data
2	$R_T = 2 \times R_T$
3	$R_T = 20 \times R_T$
4	$N_g = 3 \times N_g$
5	$X_g = X_g/2$

The only results that do not show the same values appear for the SFFOR in test 5, though the reason for these differences was not found. In the BFR, while all values differ from the results given by FLASH, they never do so with a difference higher than 11%.

2) *Influence of the calculation methods*

It is possible to see through the results of the various tests that each methodology presents different results. In the calculation methods, the use of the IEEE-D, which corresponds to considering the variation of exposure in SFFOR and the dominant phases in BFR, leads to higher values for the BFR, with a tendency for higher differences in tower type 1, when compared with the base methodology. For the SFFOR only tower type 1 shows higher values (of 47%), while all other tower types show lower values, with differences from 5% to 13% (Appendix Table B). It is considered that the difference in the response of tower type 1 is due to its different geometry, when compared to the other tower types which show a more similar structure.

For the calculation of the critical current of the BFR (Appendix Table C), the CIGRÉ method shows higher values (with differences from 1% to 21%) when compared with the original values, with the only exception being for test 3 in tower type 1, and tests 2 and 3 for other tower types. In these tests the high footing resistance causes the opposite effect, leading to lower values, from 54% in tower type 1 to 95% in other tower types for test 3 and from 16% and 21% for test 2 for tower types 2, 3, and 4. The differences that occur for these two types of tests are due to the fact that for the CIGRÉ approach, the elevation of the footing resistance leads to a raise in the critical current, which will result in a lower value of the BFR, as shown in Fig. 7 and Fig. 8.

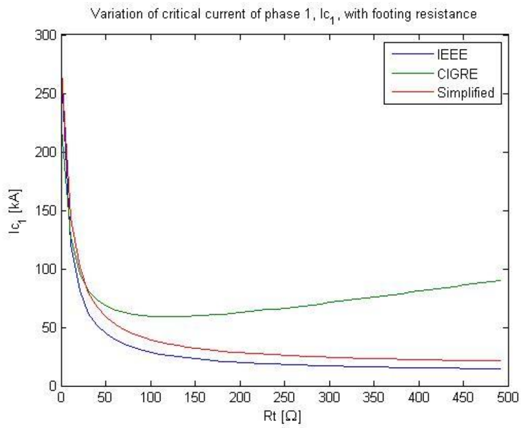

Fig. 7. Variation of the critical current with the footing resistance, for the IEEE, CIGRÉ and Simplified methodologies.

For the simplified method, when compared with the IEEE method it is possible to see that there are lower values of BFR, for all tests of all tower types, between 2.9% and 33%. The exception once again occurs for tests 2 and 3, this time in tower type 1, where a slight increase of 1% occurs. These two tests in the other tower types while showing a reduction in results, show a lower percentage difference when compared with IEEE method results. Once again, it is possible to justify the difference in results through the dependence of the simplified method on the footing resistance that causes, as seen in Fig. 7, the lowering of the critical current which will, in turn, increase the value of the BFR.

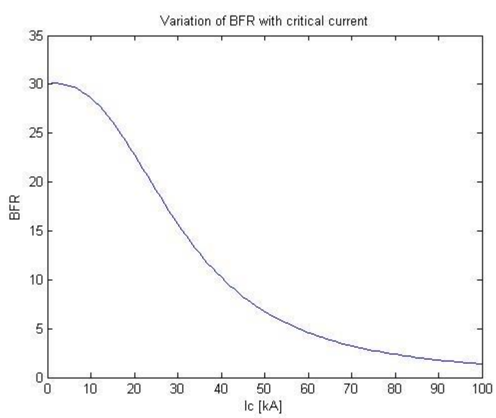

Fig. 8. Variation of BFR with the critical current.

3) Influence of the component models

For the stroke current curves, for the IEEE calculation method (Appendix Table D), while Popolansky shows higher values for SFFOR, for the BFR the results varied depending on the test and tower type. This happens due to the shapes of the curves and their variation with the stroke current. It is the opinion of this author that the IEEE curve should be preferred to the Popolansky curve, since the later was found through observations done in inappropriate sites, such as chimneys of unspecified height.

Considering the methods for the calculation of SFFOR and BFR with CIGRE method (Appendix Table E), it is possible to say that the CIGRE curve shows lower values for the SFFOR for all tests of tower type 1, and higher values for the first 4 tests of the other tower types. For the BFR, there is an inconsistence in results for different tower types. While tower type 1 shows a tendency for higher values then the IEEE-D curve, tower types 2, 3 and 4 show lower values. Tests 2 and 3 continue to be the ones that go against the norm for all tower types, having lower values for tower type 1 and higher values for the other tower types. For the Berger *et al*. methodology, all tests of all tower types show lower values for both SFFOR and BFR, with the only exception being in the BFR, once again, for test 3 of all tower types, where the high value of footing resistance lowers the critical current, and consequently raises the BFR.

For most of the other methods in study, the results show lower values than the base methodology. This tendency tends to invert as the footing resistance raises, and for tests 2 and 3 most cases show values higher than the ones for IEEE. Another notable exception occurs when we do not consider the corona effect (Appendix Table H), where the smaller radius causes an increase of the conductor and shield wire impedances, leading to lower critical currents and therefore higher values in the BFR. However, even though it generates higher values, it is not correct to disregard this effect, since it is known to be present in conductors and shield wires. Another exception is the Young *et al*. striking distance method (Appendix Table G), that seems to respond strangely to all tower types except type 1. This method shows a raise in results of 800% for tower types 2, 3 and 4, which leads to believe that this method is not well suited to these towers geometry.

It is also interesting to note that the use of soil ionization leads to lower values of the BFR in all cases (Appendix Table I). This happens due to the fact that the consideration of soil ionization leads to a lower footing resistance which, as shown in Fig. 7, leads to a higher value of critical current and consequently a lower value of BFR. As to the tower impedance, it is possible to see that for some tests there are no differences in results while for others there are lower values up to 10%, (Appendix Table J). There is some difference in responses between tower types that can be attributed to the different geometries between tower types.

VI. Conclusion

The objective of this work was to understand the differences between all the proposed methodologies for the calculation of the SFFOR and the BFR, and if the methodologies followed by FLASH were the most correct, and showed the best results, between all the methodologies and models proposed by different authors. Since there are many methodologies, a computer program called LIPE, was created, in order to facilitate the comparison of results. This program was tested in comparison with FLASH and found to be an acceptable approximation.

In terms of the different methodologies for the calculation of SFFOR and BFR, it is possible to say that the consideration of the phase with minimum critical current instead of the dominant phases leads to a raise in values in the BFR, while the consideration of a varying exposure leads to lower results for all tower types, except tower type 1. This shows the influence of the tower structure in the values of SFFOR. On the other hand, the different methodologies for calculating the critical current of the BFR show higher values in the BFR values for the CIGRÉ method and lower values for the simplified method, when compared with IEEE method. The exceptions to the rule occur for high values of footing resistance, which lead to a decrease in the values of the CIGRÉ method and an increase for the simplified method.

While the Popolansky curve shows higher results for the majority of the tests done, both for the SFFOR and the BFR, it is not advisable to use this curve in calculation due to the fact that it was found though experiments conducted in locations not appropriate for the study of lightning strikes. On the other hand, while the tests conducted for the Berger *et al*. curve show lower values when compared with IEEE curve, for both SFFOR and BFR, for all tests except those for high footing resistance, CIGRÉ shows lower values of SFFOR for tower type 1 and lower for the other tower types, and higher values for BFR in tower type one and lower values for other towers, with the only exceptions happening again for tests with high footing resistance. It is possible once again to see the different towers structure influence on the results, as well as the influence of the footing resistance.

In general, all the results for the other methods studied show that the IEEE method has the highest results for both SFFOR and BFR. The notable exception are the tests with high footing resistance, where the base method usually presents the lowest results. In terms of striking distance, the parameters proposed by Young *et al*. show an inconsistency in results that leads us to believe that this is not a good approach for these tower structures. It is important to note that the consideration of soil ionization leads to lower results in BFR and that not considering the corona effect leads to higher values of BFR. On the other hand, considering the tower impedance as an inductance results in either no changes or a decrease in values.

While the IEEE shows a very good approach in their methodology, with only CIGRÉ methodologies showing higher values for SFFOR and BFR, high values of footing resistance can have a serious impact on the results, and the FLASH method may be too optimistic in this situation. It is therefore advisable, that in a case like this, another method, possibly CIGRÉ, is used to compare the results in order to achieve a more accurate value.

While not considering the corona effects may lead to higher values, this approach is not advisable, as this is a known effect and should not be ignored.

The fact that the consideration of soil ionization leads to a lower value of the BFR is interesting and could be used in order to have an idea of the lower limit the values the BFR can reach. However, the user should find the higher values in order to have a better grasp on the worst possible outcomes.

At this point, while it is possible to say that both CIGRÉ and IEEE methodologies show a good approach and lead to good results, it is not possible to select one methodology as the best. To do that more testing would be required, for different types of data and towers, with more combinations between the two menu panels, “Metodologias” and “Métodos e Parâmetros”.

Acknowledgment

I would like to thank my supervisor, Professor Maria Teresa Correia de Barros, for all the help she provided and all the availability she showed during this work. I would also like to thank my friends and family for their support and help in revising this document. Finally, I have to thank my colleagues, Miguel Maldonado and João Brito, with whom I exchanged ideas and thoughts about this work.

References

[1] 1243-1997, I. S. (1997). *"IEEE Guide for Improving the Lightning Performance of Transmission Lines"*. New York.

[2] Alves, A. M. (2012). *Estimação do desempenho de linhas aéreas face a descargas atmosféricas - incorporação do carácter probabilístico da resistência de terra.* Lisbon.

[3] Anderson, J. G. (1975). Lightning Performance of Transmission Lines. Em *Transmission Line Reference Book, 345kV ans Above* (pp. 545-597). Palo Alto: Electric Power Research Institute.

[4] Anderson, R. B., & Eriksson, A. J. (March de 1980). Lightning Parameters for Engineering Aplication. *Electra*, pp. 65-102.

[5] Barros, M. T. (2011). *"Apontamentos da Cadeira de Alta Tensão"*.

[6] Chisholm, W. A. (s.d.). The IEEE Flash Program: A Structure for Evaluation of Transmission Lightning Performance.

[7] CIGRÉ. (1991). *Working Group 01 (Lightning), Study Comitee 33 (Overvoltages and Insulation Co-ordination), "Guide to Procedures for Estimating the Lightning Performance of Transmission Lines"*.

[8] Correia de Barros, M. T., Festas, J., Milheiras, H., Felizardo, N., & Fernandes, M. (s.d.). *Methodologies for evaluating the lightning performance of transmission lines.*

[9] IEEE. (April 1985). Working Group on Estimating the Lightning Performance of Transmission Lines, "A Simplified Method for Estimating Lightning Performance of Transmission Lines". *IEEE Transactions on Power Apparatus and Systems, PAS-104*(4).

[10] Jorge, A. M. (2011). *Avaliação de sistemas de intercepção de descargas atmosféricas em linhas de transmissão de energia eléctrica.* Lisboa.

[11] Math Works. (s.d.). *Callbacks for Specific Components.* From http://www.mathworks.com/help/matlab/creating_guis/add-code-for-components-in-callbacks.html

[12] Math Works. (s.d.). *Create a SImple App Useing GUIDE.* From http://www.mathworks.com/help/matlab/creating_guis/about-the-simple-guide-gui-example.html

[13] Math Works. (s.d.). *Creating a GUI with GUIDE.* From http://www.mathworks.com/videos/creating-a-gui-with-guide-68979.html

[14] Mikropoulos, P. N., Tsovilis, T. E., & Zlitidis, D. E. (2010). *"Software Development for the Evaluation of the Lightning Performance of Overhead Transmission Lines"*.

[15] Milheiras, H. N., & Felizardo, N. M. (1997). *Desempenho de Linhas Aéreas de Alta Tensão Face a Descargas Atmosféricas.* Lisbon.

[16] Morais, M. C. (2012). *"Notas de Apoio da Disciplina de Probabilidades e Estatística"*. Lisbon.

[17] Nucci, C. A. (2010). *"A Survey on Cigre And IEEE Procedures for the Estimation of The Lightning Performance of Overhead Transmission and Distribution Lines"*. Beijing, China.

[18] Plesch, J., Hoehn, T., & Pack, S. (2014). Modelling and analysis of different representations for high voltage tower structures. *International Conference on Lightning Protection (ICLP).* Shanghai.

[19] Popolansky, F. (s.d.). Frequency Distribution Of Amplitudes of Lightning Currents. *Electra*, *22*, 139-147.

[20] Whitehead, J. T., & Chisholm, W. A. (July 1993). IEEE Working Group Report Estimating Lightning Performance of Transmission Lines II - Updates to Analytical Models. *IEEE Transactions on Power Delivery*, *8*(3).

APPENDIX

TABLE A
COMPARISON FLASH VS. LIPE - TOWER TYPE 4

	FLASH		LIPE	
	SFFOR	BFR	SFFOR	BFR
Test 1	0	1.41	0.0021	1.3978
Test 2	0	4.26	0.0021	4.1655
Test 3	0	20.92	0.0021	21.3296
Test 4	0	4.22	0.0064	4.1933
Test 5	0.21	1.57	0.2284	1.5611

TABLE B
COMPARISON BETWEEN CALCULATION METHODS FOR SFFOR AND BFR - IEEE VS. IEEE WITH INTEGRAL - TOWER TYPE 4

	IEEE		IEEE-D	
	SFFOR	BFR	SFFOR	BFR
Test 1	0.0021	1.3978	0.002	1.4315
Test 2	0.0021	4.1655	0.002	4.2541
Test 3	0.0021	21.3296	0.002	21.4905
Test 4	0.0064	4.1933	0.006	4.2946
Test 5	0.2284	1.5611	0.1983	1.6156

TABLE C
COMPARISON BETWEEN CALCULATION METHODS FOR CRITICAL CURRENT - IEEE VS. CIGRÉ VS. SIMPLIFIED METHOD - TOWER TYPE 4

	IEEE	CIGRE	Simp.
	BFR	BFR	BFR
Test 1	1.4315	1.6116	1.1190
Test 2	4.2541	3.4460	4.0741
Test 3	21.4905	1.0485	20.8699
Test 4	4.2946	4.8348	3.3571
Test 5	1.6156	1.9519	1.2948

TABLE D
COMPARISON BETWEEN STROKE CURRENT CURVES - IEEE VS. POPOLANSKY CURVE - TOWER TYPE 4

	IEEE		Popolansky	
	SFFOR	BFR	SFFOR	BFR
Test 1	0.0021	1.3978	0.006	1.8001
Test 2	0.0021	4.1655	0.006	4.1360
Test 3	0.0021	21.3296	0.006	16.9475
Test 4	0.0064	4.1933	0.0181	5.4004
Test 5	0.2284	1.5611	0.3709	1.9426

TABLE E
COMPARISON BETWEEN STROKE CURRENT MODELS FOR METHODS WITH INTEGRAL - IEEE VS. CIGRÉ VS. BERGER *ET AL.* - TOWER TYPE 4

	IEEE-D		CIGRÉ		Berger *et al.*	
	SFFOR	BFR	SFFOR	BFR	SFFOR	BFR
Test 1	0.0021	1.3978	0.0032	0.9142	1.45E-04	0.2640
Test 2	0.0021	4.1655	0.0032	4.3705	1.45E-04	2.3104
Test 3	0.0021	21.3296	0.0032	22.6207	1.45E-04	23.128
Test 4	0.0064	4.1933	0.0096	2.7425	4.34E-04	0.7921
Test 5	0.2284	1.5611	0.1978	1.1491	0.0976	0.3580

TABLE F
COMPARISON BETWEEN DIFFERENT COLLECTION RATE CALCULATION METHODS - IEEE VS. ANDERSON VS. RIZK - TOWER TYPE 4

	IEEE-Eriksson	Anderson	Rizk
	BFR	BFR	BFR
Test 1	1.3978	0.8352	1.0468
Test 2	4.1655	2.5426	3.1194
Test 3	21.3296	13.0196	15.9733
Test 4	4.1933	2.5596	3.1403
Test 5	1.5611	0.9348	1.1574

TABLE G
COMPARISON BETWEEN DIFFERENT STRIKING DISTANCE PARAMETERS - TOWER TYPE 4

	Base	IEEE 97	Armst.	Young	Brown	Love	Wagner	Whit.
	SFFOR	SFFOR	SFFOR	SFFOR	SFFOR	SFFOR	SFFOR	SFFOR
Test 1	0.0021	7.28E-05	9.83E-04	0.0198	0.0014	0.0016	0.0014	0.0011
Test 2	0.0021	7.28E-05	9.83E-04	0.0198	0.0014	0.0016	0.0014	0.0011
Test 3	0.0021	7.28E-05	9.83E-04	0.0198	0.0014	0.0016	0.0014	0.0011
Test 4	0.0064	2.18E-04	0.0029	0.0595	0.0042	0.0049	0.0041	0.0033
Test 5	0.2284	0.1915	0.1363	3.74E-04	0.1663	0.0309	0.1026	0.0351

TABLE H
COMPARISON BETWEEN THE METHODS WITH AND WITHOUT CORONA EFFECT - TOWER TYPE 4

	With		Without	
	SFFOR	BFR	SFFOR	BFR
Test 1	0.0021	1.3978	0.0035	2.2397
Test 2	0.0021	4.1655	0.0035	6.5632
Test 3	0.0021	21.3296	0.0035	24.4991
Test 4	0.0064	4.1933	0.0104	6.7192
Test 5	0.2284	1.5611	0.2348	2.2352

TABLE I
COMPARISON BETWEEN THE METHODS WITH AND WITHOUT SOIL IONIZATION - TOWER TYPE 4

	With	Without
	BFR	BFR
Test 1	1.3250	1.3978
Test 2	3.5199	4.1655
Test 3	9.0398	21.3296
Test 4	3.9751	4.1933
Test 5	1.4796	1.5611

TABLE J
COMPARISON BETWEEN RESISTIVE AND INDUCTIVE TOWER IMPEDANCE - TOWER TYPE 4

	R	X
	BFR	BFR
Test 1	1.3978	1.3463
Test 2	4.1655	3.8373
Test 3	21.3296	21.3296
Test 4	4.1933	4.0388
Test 5	1.5611	1.5363